

## A Detailed Study on the Growth of Thin Oxide Layers on Silicon Using Ozonated Solutions

F. De Smedt,<sup>a</sup> C. Vinckier,<sup>a</sup> I. Cornelissen,<sup>b</sup> S. De Gendt,<sup>b</sup> and M. Heyns<sup>b</sup>

<sup>a</sup>Department of Chemistry, Physical and Analytical Chemistry, Katholieke Universiteit Leuven, B-3001 Heverlee, Belgium

<sup>b</sup>IMEC, B-3001 Heverlee, Belgium

The oxidation of silicon using ozonated, deionized water solutions was investigated as a function of several parameters: reaction time, pH, ozone concentration, temperature, and influence of anions. The oxidation of silicon was dependent on ozone concentration especially near neutral pH. This concentration dependence disappears at concentrations greater than 15 mg/L ozone. No temperature effect was found between 20 and 50°C. Lowering the pH leads to a less pronounced concentration dependence with no specific anion effect between HCl or HNO<sub>3</sub>. The oxidation of silicon by ozonated solutions does not lead to extensive roughening of the silicon surface as shown by atomic force microscopy measurements. Various thermal oxidation models were evaluated and the Fehner expression represents the experimental data fairly well. The overall oxidation thus follows logarithmic growth kinetics. It is proposed that ozone dissociates at the SiO<sub>2</sub>/liquid interface in a one-step reaction forming the oxidizing species, namely, O<sup>-</sup>. This radical diffuses through the SiO<sub>2</sub> layer under the influence of an electric field which develops over the oxide layer. The field-imposed drift is the limiting factor in the oxidation process. The bulk chemistry of the ozonated solutions is of no importance to the oxidation of silicon. The initial oxidation rate, defined at an oxidation time of 6 s, was dependent on the ozone concentration below 15 mg/L and leveled off above this concentration as it was limited by the field-imposed drift of the oxidation precursor. © 2000 The Electrochemical Society. S0013-4651(99)06-013-9. All rights reserved.

Manuscript submitted June 1, 1999; revised manuscript received October 14, 1999.

In the microelectronics industry the growth of ultrathin oxide layers on silicon wafers is becoming more and more important, *e.g.*, the formation of gate oxides between 1.5 and 3 nm<sup>1</sup> which is typically achieved with thermal oxidation. Growth of thin, passivating oxides is also part of the (wet) chemical cleaning processes during pregate cleaning of silicon wafers.

The oxidation of silicon at relatively low temperatures has been for many years a subject of intensive study, for example, the thermal and plasma oxidation (afterglow, anodization).<sup>2-13</sup> The kinetics and mechanism of the reaction of oxygen molecules (O<sub>2</sub>), oxygen atoms (O<sup>\*</sup>), or anions (O<sup>-</sup>) with silicon have been widely studied over the years and have resulted in several oxidation models, *e.g.*, the Deal-Grove,<sup>14</sup> Cabrera-Mott,<sup>15</sup> and Peeters-Li<sup>2,3</sup> models.

The Deal-Grove model, developed to explain the thermal oxidation of silicon by oxygen (dry or in a water ambient),<sup>14</sup> is based on an oxidation mechanism consisting of three consecutive steps: transport of the oxidizing species from the gas phase toward the SiO<sub>2</sub>-layer, diffusion through the oxide toward the SiO<sub>2</sub>/Si interface (second step), and the oxidation (third step). This resulted in a linear-parabolic growth equation of Deal-Grove (DG)

$$t_{\text{ox}}^2 + At_{\text{ox}} = B(t + \tau) \quad [1]$$

where  $t_{\text{ox}}$  is the oxide layer thickness,  $t$  the oxidation time, and  $\tau$  a shift in the time-axis. A and B are the fitting parameters.

Solving Eq. 1 results in the following expression for the oxide layer thickness,  $t_{\text{ox}}$ , as a function of time

$$\frac{t_{\text{ox}}}{A/2} = \sqrt{1 + \frac{t + \tau}{A^2/4B}} - 1 \quad [2]$$

At short oxidation times  $t + \tau \ll A^2/4B$ , Eq. 1 can be reduced after a Taylor expansion to  $At_{\text{ox}} = B(t + \tau)$  and thus a linear growth rate is observed. For longer oxidation times,  $t \gg A^2/4B$ , Eq. 1 can be simplified to  $t_{\text{ox}}^2 = Bt$ .

Another well-known oxidation model is the Cabrera-Mott model,<sup>15</sup> which provides a general theoretical frame for the oxidation of metals exposed to oxygen at low and high temperatures. For the low-temperature range the oxidation is initially extremely fast but drops within a few minutes or hours, depending on the nature of the metal, to very low or negligible values. The hypothesis proposed to explain this behavior is as follows: a strong electric field  $E$  is set up in the oxide film caused by a contact potential difference between the metal and the adsorbed oxygen. By thermionic emission or the

tunneling effect, electrons pass through the oxide from the metal to the adsorbed oxygen which is transformed into O<sup>-</sup>. This concept resulted in the following oxide growth equation with  $C$  and  $D$  fitting parameters

$$\frac{1}{t_{\text{ox}}} = C - D \ln(t) \quad [3]$$

Based on the Cabrera-Mott theory (CM) where cations migrate under the influence of a field across the growing oxide, Fehner and Mott later on published an expanded theory for low-temperature oxidation of metals.<sup>16</sup> The CM theory needed to be expanded to include anion migration through the oxide film, because the kind of ionic migration depends on the nature of the oxide. If the oxide is a network former, migration occurs through anion movement, while for network modifiers cations migrate. As silicon is a network former the oxidation involves anion migration.

In the Fehner formalism, diffusion based on a concentration gradient is not the only transport mechanism through the oxide film. Also the so-called field-imposed drift, where anions can migrate through the oxide film under the influence of an electrical field, is at play. This field over the oxide layer remains constant during the oxidation and thus limits the transport of the anions.

Under the steady-state assumption and with neglect of diffusive transport of the O<sup>-</sup> ions in comparison with field-imposed drift, logarithmic kinetics were derived, with  $E$  and  $F$  fitting parameters

$$t_{\text{ox}} = E \ln(1 + Ft) \quad [4]$$

Peeters and Li came to the same mathematical formalism, derived from their study on the plasma anodization of silicon at constant current where the oxidizing species is O<sup>-</sup>.<sup>3</sup> Recently silicon is also being thermally oxidized by ozone in order to grow (ultra)thin silicon dioxide layers.<sup>13</sup> Despite many experimental and theoretical studies of the oxidation process in the gaseous phase, in past years the use of ozone in the liquid phase has gained interest for growing thin passivating oxides in wet cleaning processes.<sup>17</sup> One of the advantages of the use of ozone is that it is a good alternative for the SPM-cleaning step (sulfuric acid peroxide mixture: H<sub>2</sub>SO<sub>4</sub>/H<sub>2</sub>O<sub>2</sub>/H<sub>2</sub>O), currently applied for the removal of residues of organic contamination whereby a passivating SiO<sub>2</sub> layer is grown on the silicon wafer.<sup>18</sup> This SPM cleaning step however causes an environmental problem because of the production of contaminated concentrated sulfuric acid as waste, and moreover, a large consumption of rinse water is needed. To allow

more environmentally and cost-friendly production, the microelectronics industry is looking for an alternative to replace sulfuric acid in the cleaning process. Due to its high oxidizing potential  $E_0 = 2.08$  V,<sup>19</sup> ozone is considered a valid alternative in wet cleaning processes. Either for the removal of organic contamination on wafer surfaces,<sup>17,20-24</sup> surface passivation after HF processes,<sup>25</sup> or even resist strip and polymer removal,<sup>26</sup> the ozone treatment in the liquid phase is considered a viable alternative.

The study described in this paper is a detailed look into the growth kinetics of the silicon oxide layer by ozonated deionized water solutions. The influence of several experimental parameters was investigated such as the oxidation time, pH, ozone concentration, nature of the anions, and temperature. The surface microroughness, which has a detrimental effect on the performance of the silicon devices, was also checked by means of atomic force microscopy (AFM) measurements.

The parameter pH needs to be controlled in all experiments involving  $O_3$ . Not only the ozone solubility in the liquid phase is pH-dependent,<sup>27</sup> but also its decomposition rate, especially in neutral conditions and at high pH.<sup>28-30</sup> Moreover, pH is an important parameter controlling the possible buildup of radicals in the solution, which are formed as products or intermediates of the complex decomposition mechanism of ozone.<sup>31-33</sup> These radicals could be the precursor for the oxidation process and their concentration is most certainly pH-dependent.

An oxide growth model is selected on basis of the best fitting to the oxide thickness-time data. Finally, some implications for the oxidation mechanism and oxidation precursors are discussed.

### Experimental

Silicon wafers [Wacker Siltronic, p-type, B-doped, Czochralski (CZ), <100>] were used for the oxidation experiments and for the AFM measurements. In the latter case, epitaxial wafers (0.008-0.020  $\Omega$  cm, 4  $\mu$ m thickness, and  $8 \times 10^{15}$  (P/B) dopant level) were oxidized.  $HNO_3$  70 v/v %,  $HCl$  37 v/v %,  $HF$  49 v/v % (all Ashland Chemicals, Gigabit grade) were used to either acidify the solution or to etch the  $SiO_2$  layer away. Deionized water was ultrapure quality (18 M $\Omega$  cm). Ozone was generated by a Sorbios ozone generator operating at a current of 2.5 A and an  $O_2$  flow of 2 L/min. The ozone concentration in the solution was measured with an Orbisphere ozone sensor which measures the ozone concentration electrochemically. Before each oxidation step the wafers were exposed to a cleaning sequence of SOM ( $H_2SO_4/O_3/H_2O$ )-dHF/dHCl- $O_3$ /dHCl-Marangoni dry, resulting in a hydrophilic surface.<sup>25</sup> Prior to the oxidation experiments the wafers were given an HF dip (2%) and this for 2 min. Subsequently, the hydrophobic wafers were immersed in the ozonated solution for a time  $t$  ranging from 6 s to 20 min. The oxidation was performed in a static tank with no ozone bubbling at the time of oxidation. Then the reoxidized (hydrophilic) wafers were rinsed in an overflow rinse tank for 30 s, followed by a drying procedure in the Semitool spin dryer PSC-101. Typically oxide layers of a few angstroms thick were grown. Ellipsometric and other surface analysis techniques are not accurate below the nanometer level. Therefore, a method for the determination of the thickness of the ultrathin  $SiO_2$  layers (<10 Å) was optimized and validated.<sup>34</sup> This method, which was already described in an earlier study,<sup>35</sup> is based on etching of the  $SiO_2$  layer by hydrofluoric acid followed by the determination of the silicon concentrations in the etch solutions. This was done by the molybdenum blue method,<sup>36</sup> which is a spectrophotometric analytical technique based on complex formation between the silicon in solution and a Mo oligomer. The formed charge-transfer absorber has a maximum absorbance at 800 nm which was measured with a Shimadzu UV 160A double-beam spectrophotometer. It has been shown that the oxide thickness  $t_{ox}$  (Å) is given by Eq. 5

$$t_{ox} = 0.097 \frac{[Si]_{exp} V_{etch}}{A_{ox}} \quad [5]$$

in which  $[Si]_{exp}$  is the silicon concentration in the etch solution (mg/L),  $V_{etch}$  the etch volume ( $\mu$ L), and  $A_{ox}$  ( $cm^2$ ) the HF-treated area on the wafer surface. This method allows one to determine

oxide thicknesses below 1 nm with a precision of better than 5%. It should be mentioned that silicon at low-level concentrations in HF-containing solutions can also be determined by other analytical techniques such as inductively coupled plasma mass spectrometry (ICP-MS)<sup>34</sup> or inductively coupled plasma optical emission spectroscopy (ICP-OES).<sup>37</sup>

For the statistical treatment of all the data, the statistical software package SAS<sup>38</sup> was used. The surface microroughness was evaluated by means of AFM measurements. The scan rate is 0.67 Hz and the set point 1.503 V on a Nanoscope AFM. With this surface analysis technique a three-dimensional view of the surface can be made (XYZ) where Z represents the depth scale or roughness. The measurements are made with a resolution of 1  $\mu$ m in the XY and 0.5 nm in the Z direction.  $R_a$  corresponds to the average microroughness expressed in nanometer.

### Results and Discussion

*Silicon oxidation at room temperature.*—The effects of several parameters on the oxide growth at room temperature were investigated: parameters under consideration were pH of the solution, the ozone concentration, and the nature of the anion used.

*Influence of pH.*—Silicon wafers were oxidized at pH 4.6 and 1.2. The former value is the equivalent pH of ozone/deionized water without additive where a slight acidification occurred when ozone was bubbled through the reaction vessel. It could be shown by ion chromatography (IC) that organic acids such as formic and oxalic acid were present in the solution. These organics were most probably generated by interaction of ozone with the wall of the PFA-Teflon (Per-Fluoro Alkoxy) tubing. The latter pH was achieved through addition of nitric acid. The oxidation time was varied between 6 s and 20 min. After rinsing and drying of the oxidized wafers, the oxide-layer thickness was measured using the procedure described.<sup>34</sup> For each oxidation time, two wafers were treated simultaneously.

The oxide layer initially grows fast and the oxide growth levels off at longer reaction time, as illustrated in Fig. 1 for a solution containing 1 mg/L ozone. An analogous growth profile has also been seen in other studies.<sup>17,23</sup> A few experiments were performed for oxidation times of 40 min, but the oxide layer thickness  $t_{ox}$  stayed nearly constant compared to the 20 min value.

Since no model is available which describes the oxidation of silicon in the liquid phase, some of the models derived from oxidation studies in the gaseous phase were tested on these experimental data. One of the most prominent models to test is the DG model. When Eq. 1 was applied to the data of Fig. 1, no values of parameters  $A$  and  $B$  could be obtained, since the convergence criterion of the fitting routine was not met. The fact that the DG formalism cannot be applied may be seen as a first indication that the transport of oxidizing species through the  $SiO_2$  layer is not solely diffusion-controlled. In

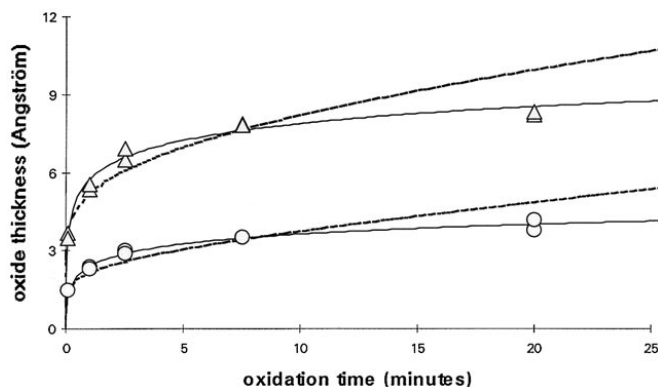


**Figure 1.** Growth profiles of  $SiO_2$  under the following experimental conditions: 1 mg/L ozone,  $T = 22^\circ C$ , and pH (○) 4.6 and 1.2 (△, nitric acid), (—) the fit based on the Fehner expression (Eq. 4) and (---) the CM formalism (Eq. 3).

this way the role for uncharged species like oxygen or ozone as the oxidation precursors becomes unlikely. This could already be expected when evaluating their diffusion through the SiO<sub>2</sub> layer. When assuming that ozone itself oxidizes silicon to form a SiO<sub>2</sub> network, the diffusion length of ozone through the SiO<sub>2</sub> layer within a certain time can be estimated. Indeed, one can calculate that at room temperature the diffusion of oxygen through SiO<sub>2</sub> is already extremely slow, since only a diffusion length of  $7 \times 10^{-3}$  Å can be achieved after 20 min ( $D_{O_2,293K} = 2.1 \times 10^{-24}$  cm<sup>2</sup>/s<sup>39</sup>). Ozone with a higher molar mass will diffuse even slower.

Some authors do claim the applicability of the CM formalism for the growth of oxide layers in ozonated solutions.<sup>23</sup> Subsequently the data were fitted to Eq. 3 of the CM model. It is obvious that Eq. 3, represented by the dotted line in Fig. 1, is not a good fit because it overpredicts  $t_{ox}$  at long oxidation times. The argument against the CM formalism is that no cation migration occurs during the oxidation of silicon but it is rather the oxidizing species which migrates toward the SiO<sub>2</sub>/Si interface. Isotope marker experiments for gas-phase oxidation indeed have shown that O<sup>-</sup> migrates through the oxide layer toward the silicon bulk and not silicon atoms toward the SiO<sub>2</sub> gas interface.<sup>40</sup>

Finally, when the experimental data were fitted to Eq. 4, a very good agreement between the model and the experimental data was obtained, as is shown by the solid lines in Fig. 1. The oxidation should then be explained through a field-imposed drift mechanism of anions through the SiO<sub>2</sub> layer toward the SiO<sub>2</sub>/Si interface. Possible oxidation precursors are thus all anions present at the SiO<sub>2</sub>/liquid interface, e.g., OH<sup>-</sup>, O<sub>2</sub><sup>-</sup>, O<sub>3</sub><sup>-</sup>, O<sup>-</sup>, ... Since reference experiments with O<sub>2</sub> saturated solutions at various pH values proved that the silicon wafers could not be oxidized in the time scale considered, the hydroxyl anion or the dissolved oxygen can be excluded as a direct precursor for silicon oxidation.

From Fig. 1, it is clear that the oxide thickness is dependent on pH with a factor of two higher at pH 1.2 than at pH 4.6. As shown in the next section, the oxide is always somewhat thicker at low pH, but except for the 1 mg/L data, this difference is minor and thus one may conclude that there is only a weak pH effect on the final oxide thickness which can be grown. Although the ozone decay rate increases at higher pH, thus forming more radical species in the course of a complex decay process,<sup>31-33</sup> e.g., HO<sub>3</sub> and HO<sub>2</sub>, no enhancement of the final oxide thickness is obtained at higher pH. This is an important indication that radicals or anions from the bulk of the solution are not directly involved in the oxidation process. The chemistry of ozone in the bulk is thus of no relevance to the oxidation process. Moreover, at low pH, where the oxidation goes somewhat faster, less anionic species are available. This is due to a shift in the chemical equilibria vs. the protonation of the anions<sup>41-43</sup>



A variation of the pH between 1.2 and 4.6 changes the H<sup>+</sup> concentration with a factor of 2500. This should strongly influence the O<sub>3</sub><sup>-</sup> and O<sub>2</sub><sup>-</sup> concentrations in the solution. Since the pH has only a minor effect on oxidation, the anions present in the bulk can also be excluded as oxidation precursors.

*Influence of the ozone concentration.*—Growth profiles were also measured for other ozone concentrations at pH 1.2 and pH 4.6. From Fig. 2 and 3 it can also be seen that the Fehnlér expression (Eq. 4) fits the data reasonably well as the oxide thicknesses are predicted within 4%. The results of the fitting are also summarized in Tables I and II.

The Fehnlér expression (Eq. 4) contains two fit parameters. As seen in Tables I and II, the parameter  $E$  can be calculated quite accurately, but parameter  $F$  carries a large uncertainty range, especially at larger ozone concentrations. According to Peeters and Li the parameter  $E$  is related to the characteristic penetration depth of the oxidizing species into the oxide and  $F$  is proportional to the precursor concentration.<sup>3</sup> Parameter  $E$  remains nearly constant for all the experiments with an average of  $0.74 \pm 0.24$  Å.  $E$  can also be seen as

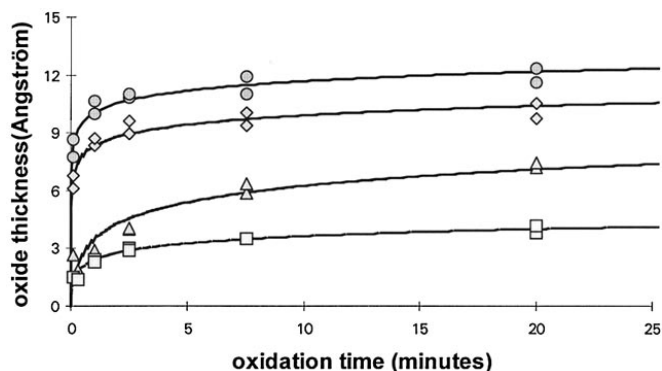


**Figure 2.** Growth profiles of SiO<sub>2</sub> as a function of the ozone concentration under the following experimental conditions:  $T = 22^\circ\text{C}$ , pH 4.6, and (□) 1, (Δ) 5, (◇) 15, and (○) 17.6 mg/L.

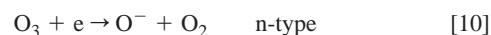
the ratio of the O<sup>-</sup> drift velocity  $v$  to the O<sup>-</sup> loss rate constant  $k$ . The experimentally derived values of  $E$  are indeed independent of the ozone concentration, as can be expected since both  $v$  and  $k$  must be assumed to be constant in the Fehnlér model.

A clear concentration dependence in the range between 1 and 18 mg/L is seen in Fig. 2 and 3:  $t_{ox,max}$ , the oxide layer thickness at 20 min, increases with the ozone concentration. Although ozone itself is not the oxidizing species, it is logical that its concentration will in some way be involved in the generation of the oxidizing precursor.

The Fehnlér model when applied to silicon is based on the theory that anions are the oxidation precursors which migrate through the oxide layer under the influence of a field over the oxide. Since the bulk chemistry does not seem to play a role in the oxidation process, the question remains how and which charged oxidizing species can be formed. One possible hypothesis is the reaction of ozone at the SiO<sub>2</sub>/liquid interface to form O<sup>-</sup> ions in the following reaction sequence



Another possible pathway would be one in which O<sup>-</sup> ions are formed directly<sup>23</sup>



In this hypothesis a higher ozone concentration in the solution should result in a higher ozone concentration at the SiO<sub>2</sub>/liquid interface, and this enhances the O<sup>-</sup> formation rate. The dependence of the oxide growth rate and the final oxide thickness levels off because at higher ozone concentrations the oxide growth is indeed limited by the field-imposed drift, whereby the field in the growing oxide

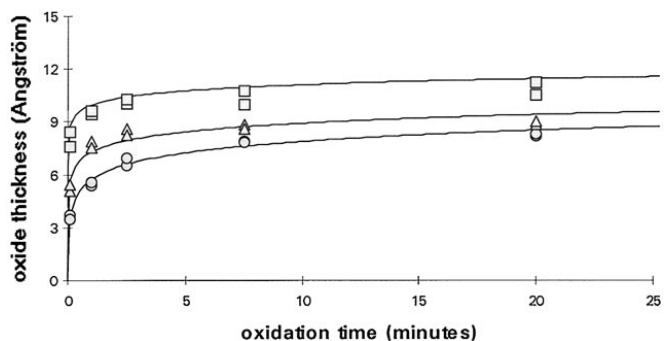


**Figure 3.** Growth profiles of SiO<sub>2</sub> as a function of the ozone concentration under the following experimental conditions:  $T = 22^\circ\text{C}$ , pH 1.2 with nitric acid as additive, and (○) 1 (Δ) 5, and (□) 15 mg/L.

**Table I. A comparison between experimental and calculated oxide thicknesses as a function of time (Eq. 4) at various initial ozone concentrations.<sup>a</sup>**

[O <sub>3</sub> ] (mg/L)	Oxidation time (min)	Experimental oxide thickness (Å)	<i>E</i> (Å)	<i>F</i> (s <sup>-1</sup> )	Calculated oxide thickness (Å)
1.0	0.1	1.47 <sup>b</sup>	0.54 ± 0.04	81.9 ± 35.8	1.20
	1	2.31 ± 0.08			2.38
	2.5	2.95 ± 0.07			2.88
	7.5	3.50 ± 0.02			3.48
	20	3.98 ± 0.31			4.01
5.0	0.1	2.27 ± 0.52	1.24 ± 0.20	15.1 ± 10.6	1.14
	1	2.90 <sup>b</sup>			3.44
	2.5	4.00 ± 0.03			4.54
	7.5	6.11 ± 0.34			5.88
15.0	20	7.31 ± 0.17	0.70 ± 0.08	(14 ± 20) 10 <sup>4</sup>	7.09
	0.1	6.44 ± 0.49			6.68
	1	8.50 ± 0.26			8.36
	2.5	9.27 ± 0.48			8.93
	7.5	9.69 ± 0.48			9.70
17.6	20	10.12 ± 0.57	0.71 ± 0.08	(14 ± 23) 10 <sup>5</sup>	10.39
	0.1	8.21 ± 0.61			8.41
	1	10.32 ± 0.49			10.11
	2.5	10.90 ± 0.13			10.70
	7.5	11.44 ± 0.64			11.48
	20	12.00 ± 0.51			12.17

<sup>a</sup> Experimental conditions pH 4.6 and room temperature.

<sup>b</sup> Only one wafer measured.

remains constant. Besides the fact that the field is limited, O<sup>-</sup> ions are lost by a mechanism which until now remains unknown<sup>3</sup> and which effect increases with increasing oxide thickness.

*Influence of the anion.*—It is known that chloride ions have a strong influence on the ozone decay rate in solution. This is because chloride anions react with ozone<sup>44</sup>

**Table II. A comparison between experimental and calculated oxide thicknesses as a function of time (Eq. 4) at various initial ozone concentrations and additive.<sup>a</sup>**

[O <sub>3</sub> ] (mg/L)	Oxidation time (min)	Experimental oxide thickness (Å)	<i>E</i> (Å)	<i>F</i> (s <sup>-1</sup> )	Calculated oxide thickness (Å)
Nitric acid					
1.0	0.1	3.58 ± 0.15	0.93 ± 0.05	460 ± 190	3.60
	1	5.46 ± 0.13			5.72
	2.5	6.70 ± 0.29			6.59
	7.5	7.84 ± 0.04			7.62
	20	8.26 ± 0.08			8.53
5.0	0.1	5.25 ± 0.25	0.71 ± 0.08	(28 ± 36) 10 <sup>3</sup>	5.65
	1	7.69 ± 0.26			7.29
	2.5	8.41 ± 0.24			7.94
	7.5	8.74 ± 0.17			8.72
15.0	20	8.95 ± 0.15	0.50 ± 0.10	(44.7 ± 148) 10 <sup>7</sup>	9.42
	0.1	7.99 ± 0.59			8.81
	1	9.53 ± 0.10			9.9
	2.5	10.15 ± 0.19			10.42
	7.5	10.36 ± 0.53			10.97
	20	10.87 ± 0.54			11.45
Hydrochloric acid					
5	0.1	5.16 ± 0.09	1.04 ± 0.07	1280 ± 650	5.04
	1	7.33 ± 0.16			7.41
	2.5	8.38 ± 0.49			8.38
	7.5	9.15 ± 0.41			9.52
	20	10.87 ± 0.34			10.54
15	0.1	8.17 ± 0.80	0.68 ± 0.10	(15.8 ± 35.4) 10 <sup>5</sup>	8.15
	1	9.98 ± 0.69			9.71
	2.5	10.15 ± 0.56			10.34
	7.5	10.64 ± 0.45			11.09
	20	12.15 ± 0.40			11.76

<sup>a</sup> Experimental conditions pH 1.2 and room temperature.

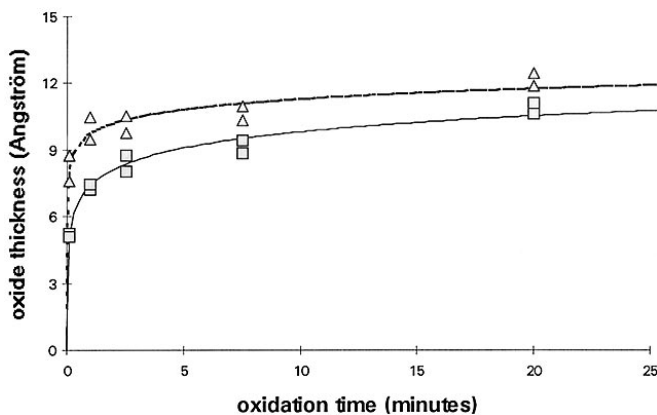
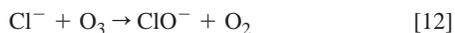


**Figure 4.** Growth profiles of SiO<sub>2</sub> as a function of the ozone concentration under the following experimental conditions:  $T = 22^\circ\text{C}$ , pH 1.2 (HCl), and (□) 5, (△) 15 mg/L.



To check the possibility that the nature of the acid (anion) is a crucial parameter in the growth mechanism, hydrochloric acid was used to acidify the solution to the same pH 1.2 as in the former experiments in nitric acid (Fig. 4).

For oxidation times shorter than 12 min, the oxide thickness is the same within 5% in HCl or HNO<sub>3</sub>. Only at an oxidation time of 20 min the oxide layer is somewhat thicker in hydrochloric acid than nitric acid. So one must conclude that there is no pronounced anion effect on the growth rate. This confirms our finding that the ozone chemistry in the bulk solution has no effect on the oxidation kinetics. Indeed, changes in the solution chemical composition due to variation of pH or additive hardly influence the growth kinetics. This indicates that the bulk of the solution and the chemical processes therein play no role but that processes at the SiO<sub>2</sub>/liquid interface should be important. There the oxidation precursor O<sup>-</sup> is formed and is subsequently transported toward the SiO<sub>2</sub>/Si interface. As already said, isotope marker studies indicated that the oxidizing species migrates through the oxide layer and thus that the oxidation occurs at the SiO<sub>2</sub>/Si interface rather than at the SiO<sub>2</sub>/liquid interface.<sup>40</sup> This mechanism is confirmed by AFM measurements which showed no roughening of the wafer surface. After a 20 min oxidation at room temperature, the surface microroughness  $R_a$  was  $0.035 \pm 0.002$  nm for 8.5 mg/L ozone at pH 4.6 (12.2 Å thick oxide) and  $0.037 \pm 0.001$  nm for 14.0 mg/L ozone at pH 1.2 (11.4 Å thick oxide). The blank, a HF-dipped wafer, had a  $R_a$  value of 0.034 nm. If oxidation had taken place at the SiO<sub>2</sub>/liquid interface one would have seen a much stronger surface roughening such as with the copper-enhanced oxidation of silicon.<sup>45</sup>

**Silicon oxidation as a function of temperature.**—Thermal oxidation of silicon is characterized by a strong positive temperature effect on the oxidation rate. When seen as an Arrhenius temperature dependence,  $e^{-E/RT}$ , values for the activation energy  $E$  in the range of 190 kJ/mol were found.<sup>14</sup> In order to check the effect of temperature on the oxidation of silicon in ozonated solutions, silicon wafers were oxidized in an HCl spiked bath (pH 1.2) at various solution temperatures in the range 20–50°C with a quasi constant ozone concentration of about 15 mg/L.

No pronounced temperature effect (positive or negative) could be observed in the range from 20 to 50°C as seen in Fig. 5. This again confirms that the bulk chemistry of ozone is irrelevant for the oxidation process. The ozone decay rate is temperature dependent, namely, an increasing temperature leads to a higher decomposition rate and thus to more radical production.<sup>46</sup> Also, the equilibrium constants for the protonation reactions (6 and 7) of the anionic species mentioned previously are temperature dependent. Besides the decay rate, the diffusion of the oxidizing species in the solid phase is also temperature dependent. For example, the activation energy for diffu-

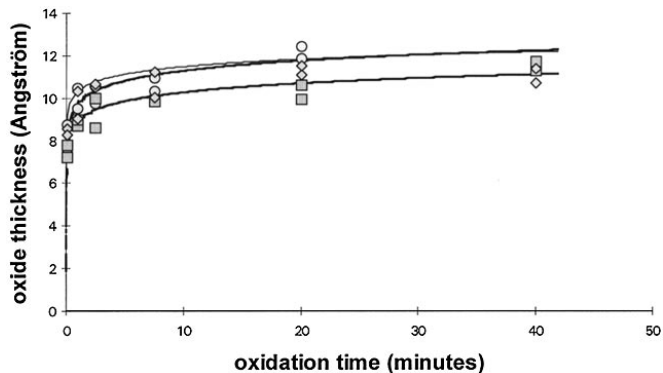


**Figure 5.** Growth profiles of SiO<sub>2</sub> as a function of temperature under the following experimental conditions: pH 1.2 (HCl), (○) 22, (□) 38, and (◇) 50°C.

sion through the SiO<sub>2</sub> layer is on the order of 113 kJ/mol for oxygen<sup>17</sup> and 77 kJ/mol for water,<sup>47</sup> explaining in part the positive temperature effect of thermal oxidation. With an activation energy of 113 kJ/mol, the diffusion becomes a factor of about 70 faster between 293 and 323 K. So even with a change in diffusion rate through the SiO<sub>2</sub> layer of almost two orders of magnitude, no temperature effect is seen on the oxidation rate and thus the diffusion of ozone or another precursor cannot be the rate-determining step.

Concerning the possible O<sup>-</sup> radical formation Reactions 8–11, one can argue that the two-step reaction sequence 8–9 is not very probable because of the endothermicity of Reaction 8 of about 105 kJ/mol. The one-step reaction at the SiO<sub>2</sub>/liquid interface is exothermic for about 40 kJ/mol. Based on the fact that no temperature dependence is seen, the one-step O<sup>-</sup> formation, Reaction 11, is proposed as the most likely one. The fact that Reaction 8, the self-decomposition of ozone, is not responsible for the oxidation is again an indication that bulk processes play no role.

From this discussion it must be concluded that the electrical field over the oxide layer is the limiting factor in the transport of the oxidation precursor(s) and thus for the oxide growth. This confirms the assumption made in the Fehner formalism (Eq. 4) where diffusive transport of anions is negligible compared to field-imposed drift.

**Initial oxidation rate.**—From the experimentally determined growth curves, an initial oxidation rate  $v_{\text{ox},i}$  was calculated by extrapolation of the oxide thickness between  $t = 0$  and 6 s for various ozone concentrations at pH 4.6 and 1.2 with nitric acid and hydrochloric acid as additives (Fig. 6). A concentration dependence of the initial oxidation rate  $v_{\text{ox},i}$  is seen at low ozone concentrations as reported before.<sup>48</sup> Above 15 mg/L ozone  $v_{\text{ox},i}$  levels off to a nearly constant value. One sees that at low ozone concentrations no linear relationship between  $v_{\text{ox},i}$  and the ozone concentration is obtained. This indicates that even in the time interval of 6 s the silicon oxidation is not entirely surface-controlled. From Table II one sees that

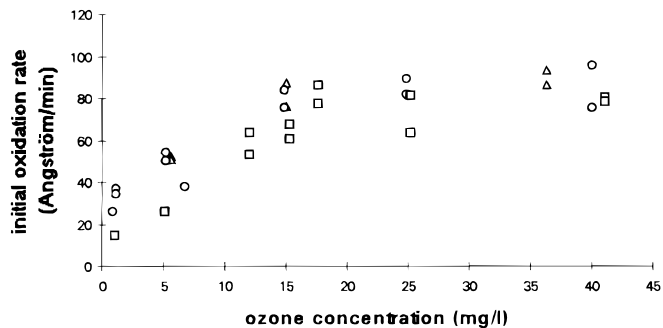


**Figure 6.** The initial oxidation rate  $v_{\text{ox},i}$  at room temperature as a function of the ozone concentration and pH (△) pH 1.2 HCl, (○) pH 1.2 HNO<sub>3</sub>, and (□) pH 4.6.

with 5 mg/L, ozone layers in the range 2.3 to 5.2 Å are grown within 6 s. Once a monolayer is formed, the field-imposed drift of the oxidation precursor, e.g., O<sup>-</sup>, becomes rate determining and not the surface reaction.

An estimation on the O<sup>-</sup>-subsurface concentration at the SiO<sub>2</sub>/liquid interface can be made from the model calculation made by Peeters and Li.<sup>3</sup> The initial oxidation rate in plasma anodization experiments at 723 and 876 K was 516 and 660 Å/min, respectively, which is about a factor of ten higher than in our experiments. The O<sup>-</sup> subsurface concentration  $N_0$  at the SiO<sub>2</sub>/liquid interface for our experiments would then be  $\leq 5 \times 10^{14}/\text{cm}^3$ . When the ozone concentration in the solution is 10 mg/L, about 0.5% of the ozone molecules needs to be converted into the O<sup>-</sup> ions at the SiO<sub>2</sub>/liquid interface in order to explain the observed initial oxidation rate in our experiments. Finally, one may notice that the kind of additive, hydrochloric or nitric acid, has no noticeable influence on the initial oxidation rate  $v_{\text{ox},i}$ , confirming our finding that the bulk chemistry is unimportant.

### Conclusions

The oxidation of silicon by means of ozonated solutions was investigated at temperatures between 22 and 50°C. The growth profile shows an initially fast growth which after a few minutes drops to a negligible value. No pronounced pH dependence is observed between 1.2 and 4.6 and no anion effect was found when using HCl and HNO<sub>3</sub>. A concentration effect was noticed in the range of 0-15 mg/L ozone. The maximum oxide thickness  $t_{\text{ox,max}}$  increases (slightly) with increasing ozone concentration. This is caused by the fact that the oxidizing species O<sup>-</sup> is formed directly from the ozone present at the SiO<sub>2</sub>/liquid interface. At higher ozone concentration this dependence disappears.

Increasing the solution temperature at constant ozone concentration does not lead to an enhanced oxidation rate. Transport of the oxidation precursor by field-imposed drift is most probably the rate determining factor of the oxidation process. At low ozone concentrations, i.e., below 15 mg/L, the initial oxidation rate  $v_{\text{ox},i}$  is dependent on the concentration but levels off at higher ozone concentrations.

The growth kinetics follow the relation  $t_{\text{ox}} = E \ln(1 + Ft)$  as proposed by Fehner as an expansion of the CM theory. An electric field is set up over the oxide layer, thus allowing the charged oxidizing species to diffuse through the SiO<sub>2</sub> layer with the field-imposed drift as limiting factor. It is proposed that this charged precursor is generated at the SiO<sub>2</sub> liquid interface where ozone forms O<sup>-</sup> in a one-step reaction. This process at the interface and the transport of O<sup>-</sup> through the SiO<sub>2</sub> layer are the rate-controlling steps, the chemistry in the bulk of the solution being of no importance.

From the processing point of view one may notice that there is no need for trying to achieve the highest possible ozone concentrations, since experiments showed that a plateau in  $t_{\text{ox,max}}$  is reached at about 15 mg/L. It is also clear that there is no need to work at elevated temperatures in ozonated solutions, as there is no benefit in increasing the temperature in terms of oxide growth.

### Acknowledgments

We thank the Funds for Scientific Research (FWO) and IMEC for their financial support. C.V. is a Research Director of FWO and F.D.S. acknowledges the Institute for Science and Technology (IWT) for a doctoral grant.

Katholieke Universiteit Leuven assisted in meeting the publication costs of this article.

### References

1. M. Depas, B. Vermeire, and M. M. Heyns, *J. Appl. Phys.*, **80**, 382 (1996).
2. J. Peeters and L. Li, *J. Appl. Phys.*, **73**, 2477 (1993).
3. J. Peeters and L. Li, *J. Appl. Phys.*, **72**, 719 (1992).
4. C. Vinckier, P. Coeckelberghs, G. Stevens, M. Heyns, and S. De Jaegere, *J. Appl. Phys.*, **62**, 1450 (1987).
5. C. Vinckier and S. De Jaegere, *J. Electrochem. Soc.*, **137**, 628 (1990).
6. J. A. Bardwell, K. B. Clark, D. F. Mitchell, D. Bisailion, G. I. Sproule, B. MacDougall, and M. J. Graham, *J. Electrochem. Soc.*, **140**, 2135 (1993).
7. W. A. Tiller, *J. Electrochem. Soc.*, **127**, 625 (1980).
8. C. J. Han and C. R. Helms, *J. Electrochem. Soc.*, **134**, 1297 (1987).
9. A. Fargeix, G. Ghibaudo, and G. Kamarinos, *J. Appl. Phys.*, **54**, 2878 (1983).
10. J. Kraiticham, *J. Appl. Phys.*, **38**, 4323 (1967).
11. A. K. Ray and A. Reisman, *J. Electrochem. Soc.*, **128**, 2460 (1981).
12. A. K. Ray and A. Reisman, *J. Electrochem. Soc.*, **128**, 2466 (1981).
13. I. W. Boyd, R. Gwilliam, and A. Kazor, *Appl. Phys. Lett.*, **65**, 412 (1994).
14. B. E. Deal and A. S. Grove, *J. Appl. Phys.*, **36**, 3770 (1965).
15. N. Cabrera and N. F. Mott, *Rep. Prog. Phys.*, **12**, 163 (1948).
16. F. P. Fehner and N. F. Mott, *Oxid. Met.*, **2**, 59 (1970).
17. T. Ohmi, T. Isagawa, M. Kogure, and T. Imaoka, *J. Electrochem. Soc.*, **140**, 804 (1993).
18. W. Kern and D. Puotinen, *RCA Rev.*, **31**, 197 (1970).
19. H. Ellis, *Book of Data, Revised Nuffield Advanced Science*, 14th ed., Nuffield-Chelsea Curriculum Trust (1996).
20. M. Kogure, T. Isagawa, T. Futatsuki, N. Yonekawa, and T. Ohmi, *Proc. Int. Environ. Sci.*, **39**, 380 (1993).
21. S. Yasui, N. Yonekawa, and T. Ohmi, *Semicond. Pure Water Conf.*, **13**, 64 (1994).
22. S. Ojima, K. Kubo, M. Kato, M. Toda, and T. Ohmi, *J. Electrochem. Soc.*, **144**, 1482 (1997).
23. S. L. Nelson, R. T. Fayfield, K. K. Christenson, and B. E. Deal, in *Proceedings of UCPSS 1996*, M. Heyns, M. Meuris, and P. Mertens, Editors, ACCO, Leuven (1996).
24. C. Kenens, S. De Gendt, D. M. Knotter, L. M. Loewenstein, M. Meuris, W. Vandervorst, and M. M. Heyns, in *Cleaning Technology in Semiconductor Device Manufacturing*, J. Ruzyllo and R. E. Novak, Editors, PV 97-35, p. 247, The Electrochemical Society Proceedings Series, Pennington, NJ (1997).
25. M. M. Heyns, M. Meuris, P. W. Mertens, H. F. Schmidt, S. Verhaverbeke, H. Bender, W. Vandervorst, M. Caymax, A. L. P. Rotondaro, Z. Hatcher, and D. Graf, in *Proceedings of the 40th Annual Technical Meeting of the Institute of Environmental Sciences*, Chicago, IL, May 1-6, 1994.
26. S. De Gendt, P. Snee, I. Cornelissen, M. Lux, R. Vos, P. W. Mertens, D. M. Knotter, M. Meuris, and M. M. Heyns, in *Solid State Phenomena (Proc. UCPSS 1998)*, Switzerland, Vol. 65-66, pp. 165-168 (1999).
27. F. De Smedt and C. Vinckier, Unpublished results (1998).
28. H. Tomiyasu, H. Fukutomi, and G. Gordon, *Inorg. Chem.*, **24**, 2962 (1985).
29. L. Forni, D. Bahnmann, and E. J. Hart, *J. Phys. Chem.*, **86**, 255 (1982).
30. J. Staehelin and J. Hoigné, *Environ. Sci. Technol.*, **16**, 676 (1982).
31. R. E. Bühler, J. Staehelin, and J. Hoigné, *J. Phys. Chem.*, **88**, 2560 (1984).
32. K. Sehested, J. Holcman, and E. J. Hart, *J. Phys. Chem.*, **87**, 1951 (1983).
33. K. Sehested, J. Holcman, E. Bjergbakke, and E. J. Hart, *J. Phys. Chem.*, **88**, 4144 (1984).
34. F. De Smedt, G. Stevens, S. De Gendt, I. Cornelissen, S. Arnauts, M. Meuris, M. M. Heyns, and C. Vinckier, *J. Electrochem. Soc.*, **145**, 1873 (1999).
35. K. Vepa, K. Baker, and L. W. Shive, in *Cleaning Technology in Semiconductor Device Manufacturing IV*, R. E. Novak and J. Ruzyllo, Editors, PV 95-20, p. 385, The Electrochemical Society Proceedings Series, Pennington, NJ (1995).
36. H. Bennett and R. A. Reed, *Chemical Methods of Silicate Analysis*, Academic Press, London and New York (1971).
37. F. Li, M. K. Balzas, and B. E. Deal, in *Proceedings of the 18th Semiconductor Pure Water and Chemicals Conference*, M. K. Balzas, Editor, p. 125, Balzas Analytical Laboratories, Santa Clara, CA (1999).
38. SAS Statistical Package, SAS Institute, Inc., Cary, NC (1989).
39. F. J. Norton, *Nature*, **171**, 701 (1961).
40. C. Fu, C. Mikhelsen, J. Schmitt, J. Abelson, J. C. Knights, N. Johnson, A. Backer, and M. J. Thompson, *J. Electron. Mater.*, **44**, 685 (1985).
41. J. Staehelin, J. Hoigné, and R. E. Bühler, *J. Phys. Chem.*, **88**, 5999 (1984).
42. J. Staehelin and J. Hoigné, *Environ. Sci. Technol.*, **19**, 1206 (1985).
43. G. Czapski, *J. Am. Chem. Soc.*, **67**, 2180 (1963).
44. J. Hoigné, H. Bader, W. R. Haag, and J. Staehelin, *Water Res.*, **19**, 993 (1985).
45. M. Börner, N. Junghans, S. Landau, and B. D. Kolbesen, *Solid State Phenomena (Proc. UCPSS 1998)*, Switzerland, Vol. 65-66, pp. 245-248 (1999).
46. J. L. Sotelo, F. J. Beltran, F. J. Benitez, and J. Beltran-Heredia, *Ind. Eng. Chem. Res.*, **26**, 39 (1987).
47. A. J. Moulson and J. P. Roberts, *Trans. Faraday Soc.*, **57**, 1208 (1961).
48. F. De Smedt, C. Vinckier, G. Gilis, I. Cornelissen, S. De Gendt, M. Meuris, and M. Heyns, *Solid State Phenomena (Proc. UCPSS 1998)*, Scitec Publications, Vol. 65-66, pp. 81-84, Switzerland (1999).